NAVAL AIR WARFARE CENTER AIRCRAFT DIVISION
PATUXENT RIVER, MARYLAND 20670-5304

TECHNICAL MEMORANDUM

REPORT NO: NAWCADPAX--96-9-TM

COPY NO. 43

ROLL ANGLE AND BALL WIDTH DATA METHOD BASED ON DYNAMIC PRESSURE FOR HELICOPTER APPLICATIONS

27 September 1996

19961028 085

Approved for public release; distribution is unlimited.

DTIC QUALITY INSPECTED 1

DEPARTMENT OF THE NAVY
NAVAL AIR WARFARE CENTER AIRCRAFT DIVISION
PATUXENT RIVER, MARYLAND 20670-5304

NAWCADPAX--96-9-TM
27 September 1996

PREPARED BY:

Herman Kolwey 9/19/96
HERMAN KOLWEY / DATE

RELEASED BY:

D. J. Krall /24 SEP 96
D. KRALL, MAJ, USMC / DATE
H53 Platform Coordinator
Naval Rotary Wing Aircraft Test Squadron
Naval Air Warfare Center Aircraft Division

T. Caudill / 19 Sep 96
T. CAUDILL, MAJ, USMC / DATE
AH1W Platform Coordinator
Naval Rotary Wing Aircraft Test Squadron
Naval Air Warfare Center Aircraft Division

9/27/96
R. GLOCKNER / DATE
Head, Aeromechanical and Flight Controls Division
Naval Air Warfare Center Aircraft Division

DISCLAIMER NOTICE

THIS DOCUMENT IS BEST QUALITY AVAILABLE. THE COPY FURNISHED TO DTIC CONTAINED A SIGNIFICANT NUMBER OF COLOR PAGES WHICH DO NOT REPRODUCE LEGIBLY ON BLACK AND WHITE MICROFICHE.

REPORT DOCUMENTATION PAGE

Form Approved
OMB No. 0704-0188

Public reporting burden for this collection of information is estimated to average 1 hour per response, including the time for reviewing instructions, searching existing data sources, gathering and maintaining the data needed, and completing and reviewing the collection of information. Send comments regarding this burden estimate only, other aspect of this collection of information, including suggestions for reducing this burden, to Washington Headquarters Services, Directorate for Information Operations and Reports, 1215 Jefferson Davis Highway, Suite 1204, Arlington, VA 22202-4302, and to the Office of Management and Budget, Paperwork Reduction Project (07804-0188), Washington, DC 20503.

1. AGENCY USE ONLY *(LEAVE BLANK)*	2. REPORT DATE	3. REPORT TYPE AND DATES COVERED
	27 SEPTEMBER 1996	TECHNICAL MEMORANDUM

4. TITLE AND SUBTITLE

ROLL ANGLE AND BALL WIDTH DATA METHOD BASED ON DYNAMIC PRESSURE FOR HELICOPTER APPLICATIONS

5. FUNDING NUMBERS

6. AUTHOR(S)

HERMAN KOLWEY

7. PERFORMING ORGANIZATION NAME(S) AND ADDRESS(ES)

DEPARTMENT OF THE NAVY
NAVAL ROTARY WING AIRCRAFT TEST SQUADRON
NAVAL AIR WARFARE CENTER AIRCRAFT DIVISION
PATUXENT RIVER, MD 20670-5304

8. PERFORMING ORGANIZATION REPORT NUMBER

NAWCADPAX--96-9-TM

9. SPONSORING/MONITORING AGENCY NAME(S) AND ADDRESS(ES)

NAVAL TEST WING ATLANTIC
NAVAL AIR WARFARE CENTER AIRCRAFT DIVISION
DEPARTMENT OF THE NAVY
PATUXENT RIVER, MD 20670-5304

10. SPONSORING/MONITORING AGENCY REPORT NUMBER

11. SUPPLEMENTARY NOTES

12a. DISTRIBUTION/AVAILABILITY STATEMENT

APPROVED FOR PUBLIC RELEASE; DISTRIBUTION IS UNLIMITED.

12b. DISTRIBUTION CODE

13. ABSTRACT *(Maximum 200 words)*

A search of MH-53E and CH-53E roll angle, ball width, and sideslip data was conducted in order to establish Fleet steady heading sideslip (SHSS) NATOPS limits for aircraft lacking nose booms. No ball width data were found for the CH-53E. Plots of the available information were sent to NAVTESTPILOTSCH (Bob Miller). He suggested that the data (three different slopes) might be normalized to one slope, using a velocity squared ratio as is done for fixed-wing aircraft. Doing this collapsed the data to a single line. An MH data plot was made (roll angle versus ball width - believed to be linear for SHSS conditions) and used to calculate CH ball width from roll angle data. AH-1W data to 125 KIAS containing ball "pegged" (against the limit of travel) points were handled similarly, allowing extrapolation to 170 KIAS. A family of curves was then generated (both course and fine) for the Cobra as a function of airspeed. Finally, lateral g sensitivity was derived from a plot of ball width versus roll angle, allowing correction of a lateral g-driven (accelerometer) ball indication in a helmet mounted display. This process is recommended for use in handling roll angle and ball width information in flight simulations. Consideration should be given to incorporating this method into the NAVTESTPILOTSCH curriculum.

14. SUBJECT TERMS		15. NUMBER OF PAGES
DYNAMIC PRESSURE "q"	ROLL ANGLE	35
STEADY HEADING SIDESLIP (SHSS)	BALL WIDTH	16. PRICE CODE
LATERAL LOAD FACTOR		

17. SECURITY CLASSIFICATION OF REPORT	18. SECURITY CLASSIFICATION OF THIS PAGE	19. SECURITY CLASSIFICATION OF ABSTRACT	20. LIMITATION OF ABSTRACT
UNCLASSIFIED	UNCLASSIFIED	UNCLASSIFIED	SAR

SUMMARY

A search through existing data for the MH-53E and CH-53E regarding roll angle and ball width as a function of sideslip in order to establish fleet steady heading sideslip (SHSS) NATOPS limits for aircraft not equipped with nose boom yielded data for both roll angle versus sideslip and ball width versus sideslip at three different airspeeds for the MH-53E. For the CH-53E, however, only roll angle versus sideslip information was found at one airspeed in clean and auxiliary tank configurations. The available information was plotted and sent to the Naval Test Pilot School (NAVTESTPILOTSCH) (Bob Miller) to see if additional data were available. Mr. Miller suggested that the data for the three airspeeds (different slopes) might be normalized to one of the airspeeds by using a velocity squared ratio, as is done for fixed-wing aircraft. This was done, collapsing the data onto a single line.

Thinking that roll angle and ball width should be consistent and linear for SHSS test conditions, a plot of these parameters was made from the MH data and used to calculate ball width from the CH roll angle information.

Data for the AH-1W were handled in a similar manner. This data contained information for conditions where the ball was "pegged" (against the limit of travel) and flown to a maximum of 125 KIAS. From the 125 KIAS test data extrapolation, 170 KIAS was made and a family of curves was generated (both course and fine) for the Cobra as a function of airspeed.

Further, knowing the relationship between ball width and roll angle allowed a determination of lateral g sensitivity for proper indication of ball width in a helmet mounted display with the ball driven by a lateral accelerometer.

This process should be used to provide data for utilization by the simulator manufacturers for roll angle and ball width information in the simulation. Consideration should be given to incorporating this method into the NAVTESTPILOTSCH curriculum.

INTRODUCTION

BACKGROUND

1. An instrumented nose boom is typically installed on test helicopters as a means of measuring sideslip and monitoring those structural loads which are a function of sideslip. Most helicopters develop a roll angle during out-of-trim flight because of aerodynamic forces on the broadside of the fuselage. In level, out-of-trim flight, known in the test community as steady heading sideslip (SHSS), roll angle and ball position will be related. Roll angle is typically instrumented, but the ball indicator, although a simple device, is not able to be instrumented and must be read and recorded in the cockpit. Unfortunately, the ball is the only indicator available to the pilot in noninstrumented fleet aircraft. The end result is data plots for flight limits as a function of sideslip angle for the test helicopter with a nose-mounted boom, but no way for fleet pilots to use the information, since they lack a sideslip indication.

2. The writer recently searched for ball width versus sideslip information for the MH-53E and CH-53E helicopters. The MH-53E, shown in figure A-1, is a derivative of the CH-53E, shown in figure A-2. The most significant external differences between the two are the auxiliary fuel tank arrangements. The CH-53E has a relatively small sponson and jettisonable external fuel tanks. The MH-53E has large nonjettisonable fuel tank sponsons. The data search produced sideslip, roll angle, and ball width data for the MH-53E at three different airspeeds, but for the CH-53E, only roll angle and sideslip data could be located for one airspeed, in both the clean and auxiliary tank configurations.

RESULTS AND DISCUSSION

3. Figures A-3 and A-4 present roll angle versus sideslip and ball width versus sideslip data, respectively, for the MH-53E at three different airspeeds. These plots were sent to Bob Miller at the Naval Test Pilot School (NAVTESTPILOTSCH) who suggested normalizing the three different airspeeds (figures A-3 and A-4) to 105 KIAS using a "q" or velocity squared ratio and trying to collapse them onto a single line (something done in the fixed-wing world, but not the helicopter community). The three airspeed lines collapsed very nicely as shown in figures A-5 and A-6.

4. Figures A-7 and A-8 show the first order least squares fit and the r^2 (correlation coefficient squared) for roll angle versus sideslip and ball width versus sideslip before q normalization. Figures A-9 and A-10 show the first order least squares fit and the r^2 for roll angle versus sideslip and ball width versus sideslip, respectively, after q normalization. Table 1 summarizes the r^2 results. Statistical correlation increased significantly after q normalization based on all the test data. It was concluded that data plots of different airspeeds (different slopes) for the same altitude can be normalized on to one plot using a velocity squared ratio (q-based) of the airspeeds with good statistical correlation.

Table 1
MH-53E SHSS DATA WITH AND WITHOUT q NORMALIZATION

	r^2 Before q Normalization (all data)	r^2 After q Normalization
Roll Angle versus Sideslip	0.7883	0.9635
Ball Position versus Sideslip	0.8582	0.9593

NOTE: r^2 values approaching 1.0 indicate a better fit to the data.

5. Thinking that a more rigorous analysis of the data was in order, the data shown in figures A-3 and A-4 were individually fitted with a straight line equation for each airspeed (two data points at 10 and 28 deg sideslip on the 80 KIAS line were deleted since they were clearly off the line). The r^2 values of the three lines were averaged for comparison with the q-adjusted plot. These results are shown in table 2 for roll and table 3 for ball width. Again, the r^2 value for the q-normalized data exceeds that of the average of the individual airspeed lines for both roll and ball width. This confirms the test method. Also, the best fit of the three airspeeds was for the 105 KIAS data set for both roll and ball width.

Table 2
MH-53E SHSS DATA (ROLL) WITH AND WITHOUT q NORMALIZATION

	r^2 Before q Normalization	r^2 After q Normalization
Roll versus Sideslip - all data together	0.7833	0.9635
Roll versus Sideslip - 80 KIAS	0.9508	
Roll versus Sideslip - 105 KIAS	0.9916	
Roll versus Sideslip - 150 KIAS	0.9514	
Average of above 3 lines	0.9646	0.9723

Table 3
MH-53E SHSS DATA (BALL) WITH AND WITHOUT q NORMALIZATION

	r^2 Before q Normalization	r^2 After q Normalization
Ball versus Sideslip - all data together	0.8582	0.9593
Ball versus Sideslip - 80 KIAS(1)	0.9889	
Ball versus Sideslip - 105 KIAS	0.9983	
Ball versus Sideslip - 150 KIAS	0.9851	
Average of above 3 lines(1)	0.9908	0.9922

NOTE: (1) Two data points (10 and 28 deg sideslip) on the 80 KIAS line were deleted as they were clearly off the line.

6. The MH-53E data range was from 80 to 150 kt at nominally 2,000 ft Hp (assumed standard day). While this data provided a large airspeed spread for examination, it did not provide any comparison data to evaluate density altitude effects. Theory indicates that density will have no effect on the q-normalized plots since:

$$q = 1/2 \times \rho_{STANDARD\ SEA\ LEVEL} \times V^2_{KCAS}$$

where $V_{KCAS} = V_{KIAS} + \Delta V_{POS} + \Delta V_{IC}$

However, q normalization could not be verified for different density conditions. Data should be acquired at 8,000 to 10,000 ft for comparison with data derived by this method at 2,000 ft.

7. Dynamic pressure normalization promises to be a valuable tool for providing fleet pilots with limits for aircraft which do not have nose booms and for comparing data taken at different airspeeds and altitudes. It also has the potential to provide the simulator data base with a more useful tool than has been previously available. This data method should be considered for incorporation into the NAVTESTPILOTSCH curriculum and used for presentation of flight test data. It should also be included in simulator criteria data reports for a more accurate simulation definition. The following factors still need to be evaluated to determine the extent of the q normalization method's utility: density altitude, GW, and CG. Side forces generated by the tail rotor increase while aerodynamic forces related to q decrease at low airspeeds. Although SHSS tests are not usually conducted on the backside of the power curve, SHSS data may be influenced by the tail rotor. It is recommended that caution be used before applying this method below bucket airspeeds.

8. While q normalization promises to enhance the productivity of flight test data, it still does not solve the original dilemma, how to relate sideslip to ball position for the CH-53E in order to provide nonnose boom equipped aircraft with structural based SHSS limits. The available CH-53E roll angle data are presented in figure A-11. Roll angle and ball position should be related (but not necessarily linear) in SHSS because the only force acting on the ball is gravity. Therefore, for a given flight condition, observed ball position is only a function of the tilt of the gauge (aircraft roll attitude), the shape of the ball race, and the observer's position. For a given type of aircraft, the shape of the ball race and the parallax introduced by the observer's viewpoint are constant. The CH-53E and the MH-53E gauges and observer positions are identical. This means that roll angle versus ball width is the same for both the CH-53E and the MH-53E. A plot of roll attitude versus ball position from MH-53E is presented in figure A-12. A first order linear regression was applied. Ball position for a given sideslip condition can now be found by:

Enter roll angle versus sideslip plot (figure A-11) with the desired sideslip condition.
Determine the roll attitude.
Enter the roll angle versus ball position plot (figure A-12) with the roll angle from figure A-11 to find ball position.

Figure A-13 presents the results of this process. It was concluded that a plot of ball width versus roll angle can be used on airframes of the same family as a "calibration plot" to derive ball width information from roll angles for SHSS conditions.

9. This method was also utilized on test data from the AH-1W (figure A-14) for SHSS test conditions. Roll and ball data were available for airspeeds of 60, 100, and 125 KIAS, as shown in figures A-15 and A-16. Since for several of the data points the ball was "pegged" (at the limit of its track) at about 2.5 ball widths, a plot was made, as was done with the CH-53E, of roll angle versus ball width (figure A-17) so that an equivalent "unpegged" ball position could be determined (as would be indicated on an expanded-range indicator). Data were then normalized to the 100 KIAS condition using the velocity squared ratio as was done before. Figures A-18 and A-19 show data normalized to 100 KIAS. Although the normalizing data at 100 KIAS for the AH-1W showed more scatter, it followed the theory and the faired line was used as a basis for extrapolating the roll and ball width data to 140, 150, 160, and 170 KIAS, generating a family of ball versus sideslip curves, as shown in figures A-20 (course) and A-21 (fine), respectively. This method can be used to determine the "equivalent" ball position beyond the point where it "pegs" because of its limited range (e.g., Cobra at 2.5 ball widths) and can be used to extrapolate roll and ball positions to airspeeds beyond the range of the available test data (e.g., test data at 60, 100, and 125 KIAS roll and ball information extrapolated up to 170 KIAS).

10. During the time period of developing this technical memorandum, a separate evaluation was being conducted of a helmet mounted display (HMD) in the CH-53E, which included a symbol for "ball width" driven by a lateral accelerometer. This symbol did not work like the one in the cockpit and, in fact, appeared to be inoperative. Calibration was found to be one ball width per g. Knowing the relationship between ball width and roll angle as determined by the method of this technical memorandum allowed a quick calculation of the lateral g sensitivity of the ball. By entering one ball width in the equation of figure A-12, you get 5.17 deg of roll at one ball width. Lateral g is given by the following equation:

$$g_{lat} = Nz \times \sin(\text{Roll Angle})$$
$$= 1 \times \sin 5.17$$
$$g_{lat} = 0.090 \text{ g/ball width}$$

Lateral g sensitivity of the ball in the MH-53E/CH-53E was determined to be 0.09 g. This order-of-magnitude correction to the ball indication in the HMD provided a match to that in the aircraft for a correct indication. Using a similar procedure for the AH-1W (figure A-17) allowed calculation of a roll angle of 3.19 deg for one ball width for a lateral g of 0.06 at one ball width. This method is recommended to provide lateral g sensitivity of the ball in aircraft equipped with HMD's or HUD's driven by a lateral accelerometer and for proper indication of lateral g in simulations. It may also be used to provide proper kinesthetic or side force cues to pilots in the simulation.

CONCLUSIONS

11. Data plots of different airspeeds (different slopes) for the same altitude can be normalized onto one plot using a velocity squared ratio (q-based) of the airspeeds with good statistical correlation (paragraph 4).

12. The r^2 value for the q-normalized data exceeds that of the average of the individual airspeed lines for both roll and ball width (paragraph 5).

13. Dynamic pressure normalization promises to be a valuable tool for comparing data taken at different airspeeds and altitudes (paragraph 7).

14. A plot of ball width versus roll angle can be used on airframes of the same family as a "calibration plot" to derive ball width information from roll angles for SHSS conditions (paragraph 8).

15. This method can be used to determine the "equivalent" ball position beyond the point where it "pegs" because of its limited range (e.g., Cobra at 2.5 ball widths) and can be used to extrapolate roll and ball positions to airspeeds beyond the range of the available test data (e.g., test data at 60, 100, and 125 KIAS roll and ball information extrapolated up to 170 KIAS) (paragraph 9).

16. Knowing the relationship between ball width and roll angle allowed a determination of lateral g sensitivity for proper indication of ball width in an HMD with the ball driven by a lateral accelerometer (paragraph 10).

17. Lateral g sensitivity of the ball was determined to be 0.09 for the MH-53E/CH-53E and 0.06 for the AH-1W (paragraph 10).

RECOMMENDATIONS

18. Data should be acquired at 8,000 to 10,000 ft for comparison with data derived by this method at 2,000 ft (paragraph 6).

19. Consider incorporating data method into the NAVTESTPILOTSCH curriculum and use for presentation of flight test data. Also include in simulator criteria data reports for a more accurate simulation definition (paragraph 7).

20. This method is recommended to provide lateral g sensitivity of the ball in aircraft equipped with HMD's or HUD's driven by a lateral accelerometer and for proper indication of lateral g in simulations. It may also be used to provide proper kinesthetic or side force cues to pilots in the simulation (paragraph 10).

THIS PAGE INTENTIONALLY LEFT BLANK

APPENDIX A
FIGURES

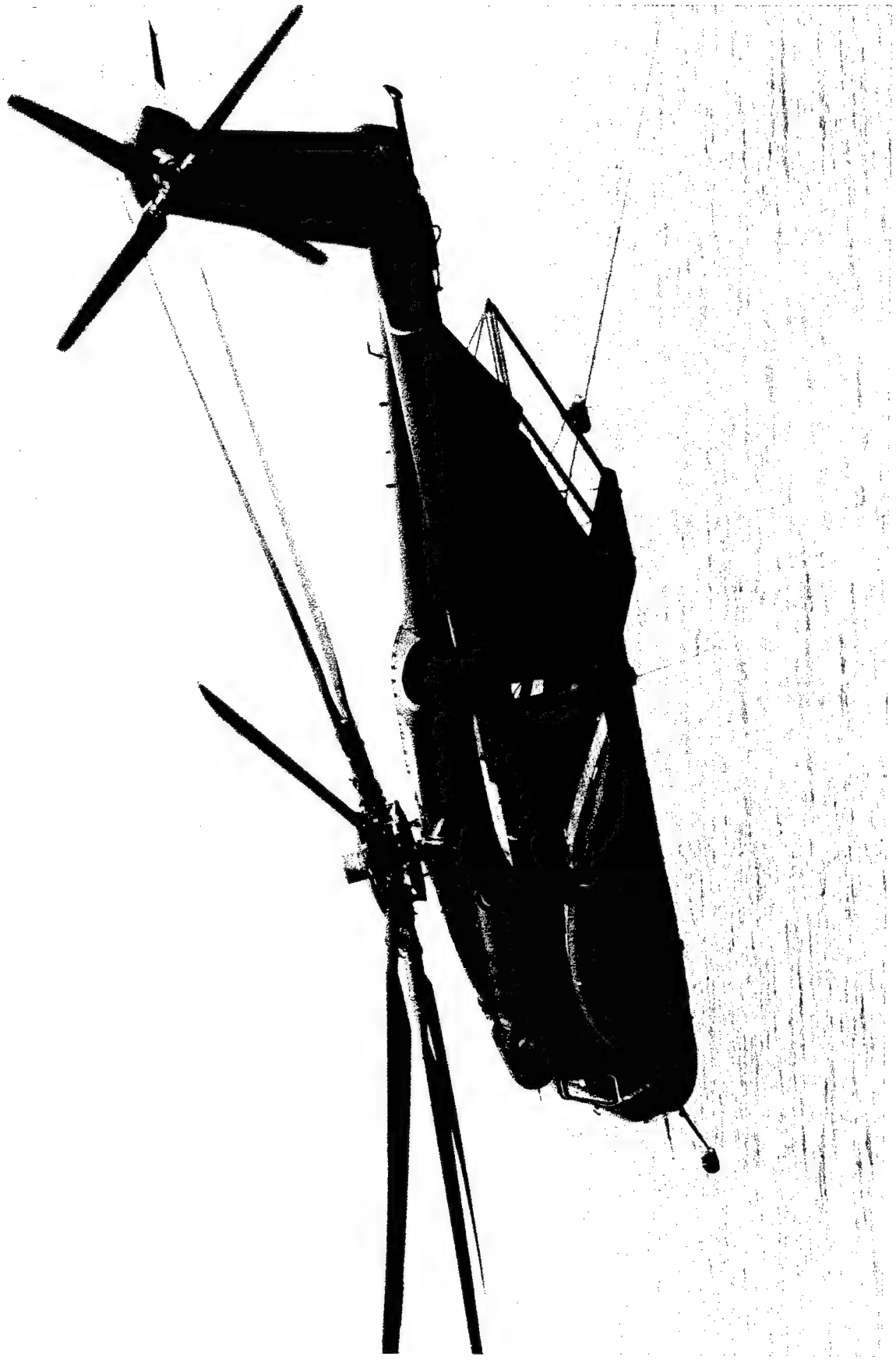

Figure A-1
MH-53E AIRCRAFT

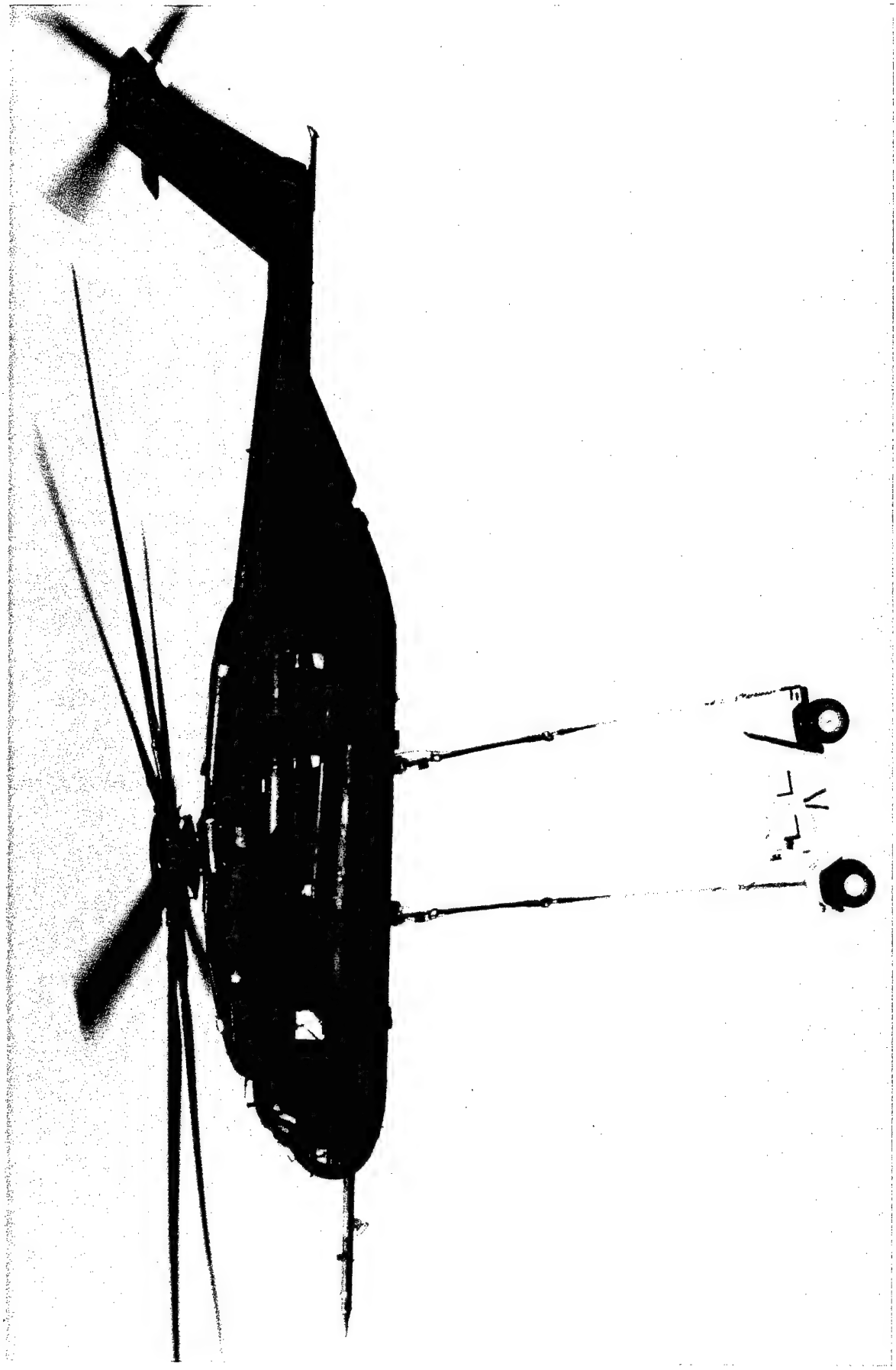

Figure A-2
CH-53E AIRCRAFT

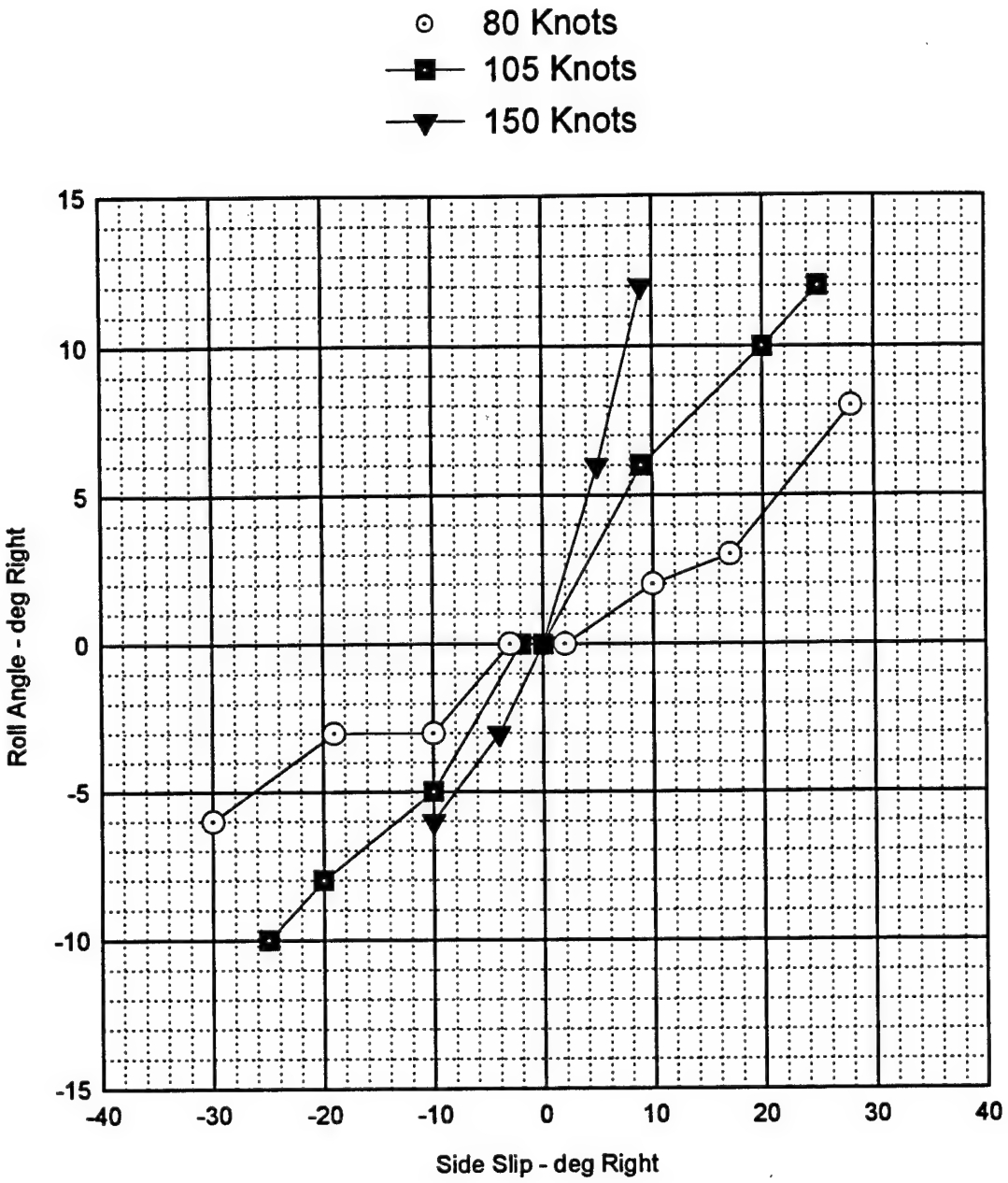

Figure A-3
MH-53E SIDESLIP VERSUS ROLL ANGLE

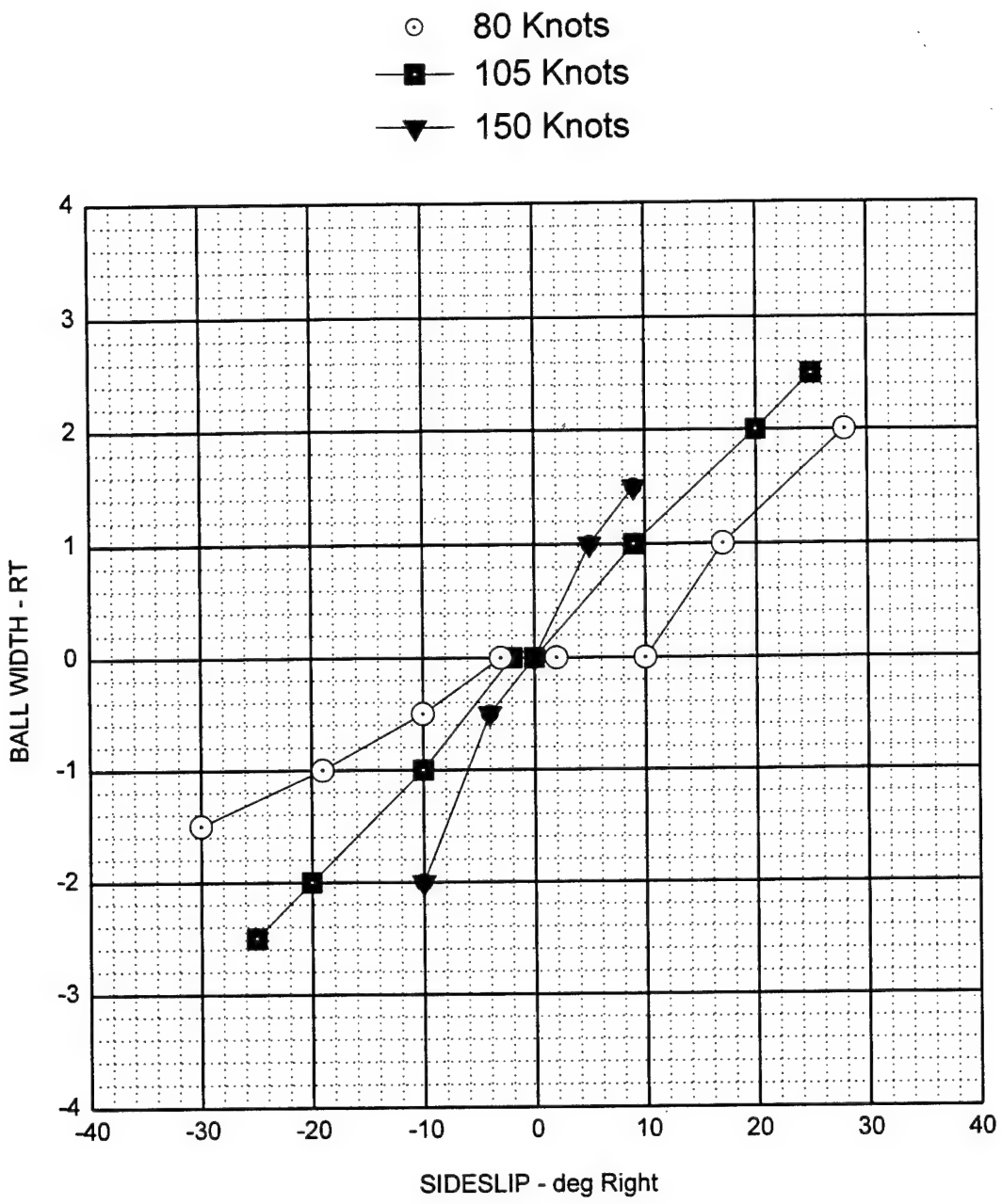

Figure A-4
MH-53E SIDESLIP VERSUS BALL WIDTH

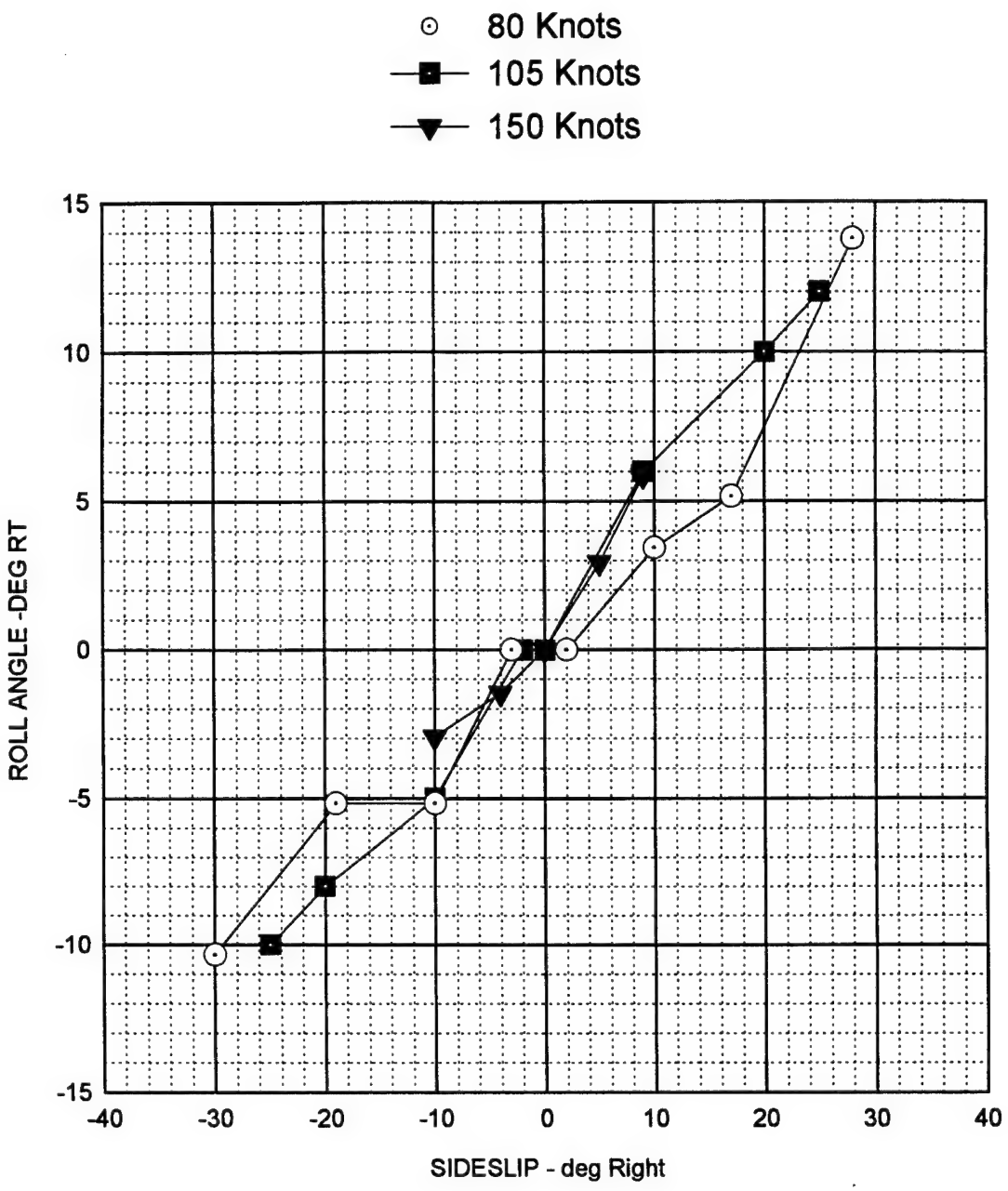

Figure A-5
MH-53E SIDESLIP VERSUS ROLL ANGLE

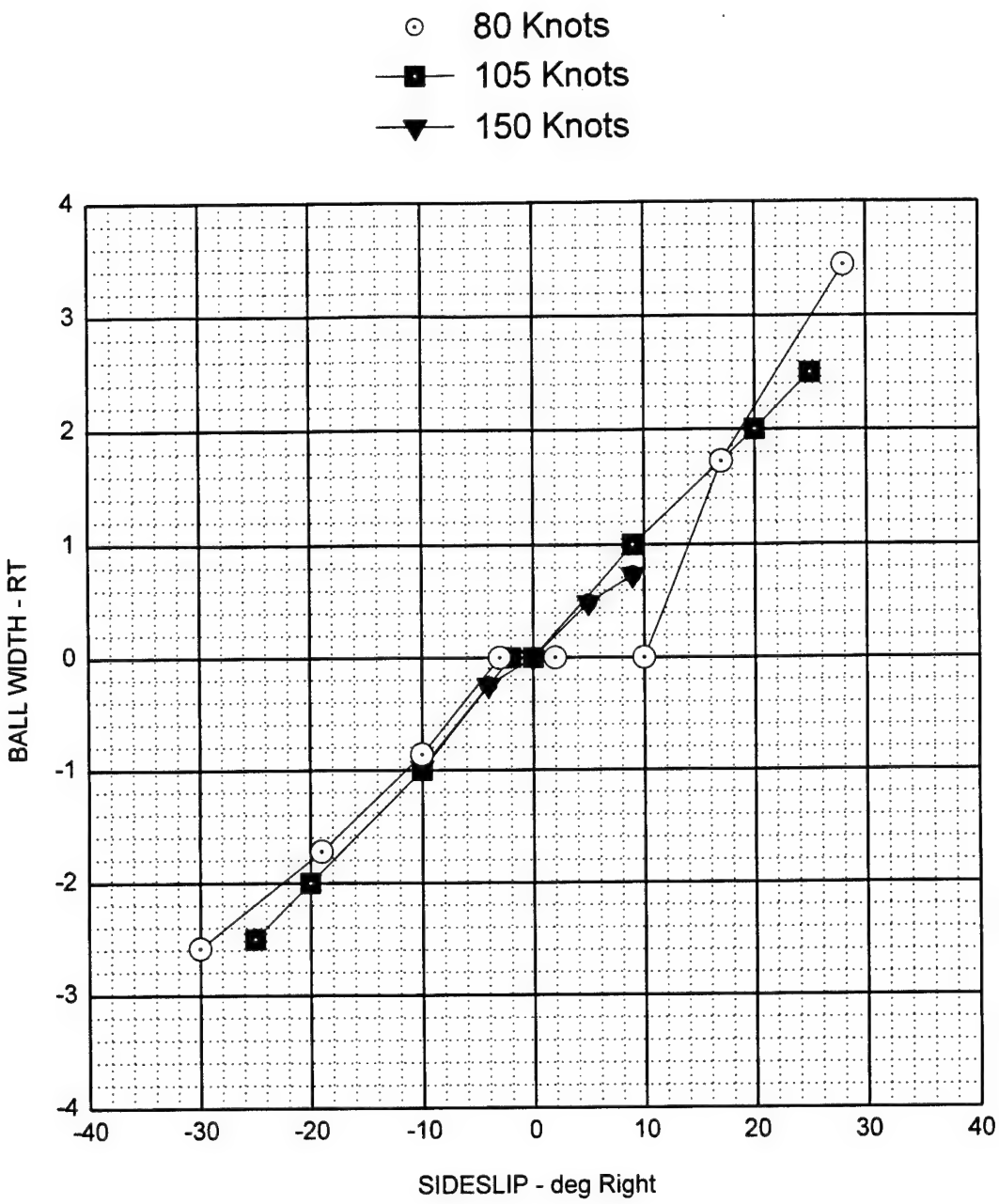

Figure A-6
MH-53E SIDESLIP VERSUS BALL WIDTH

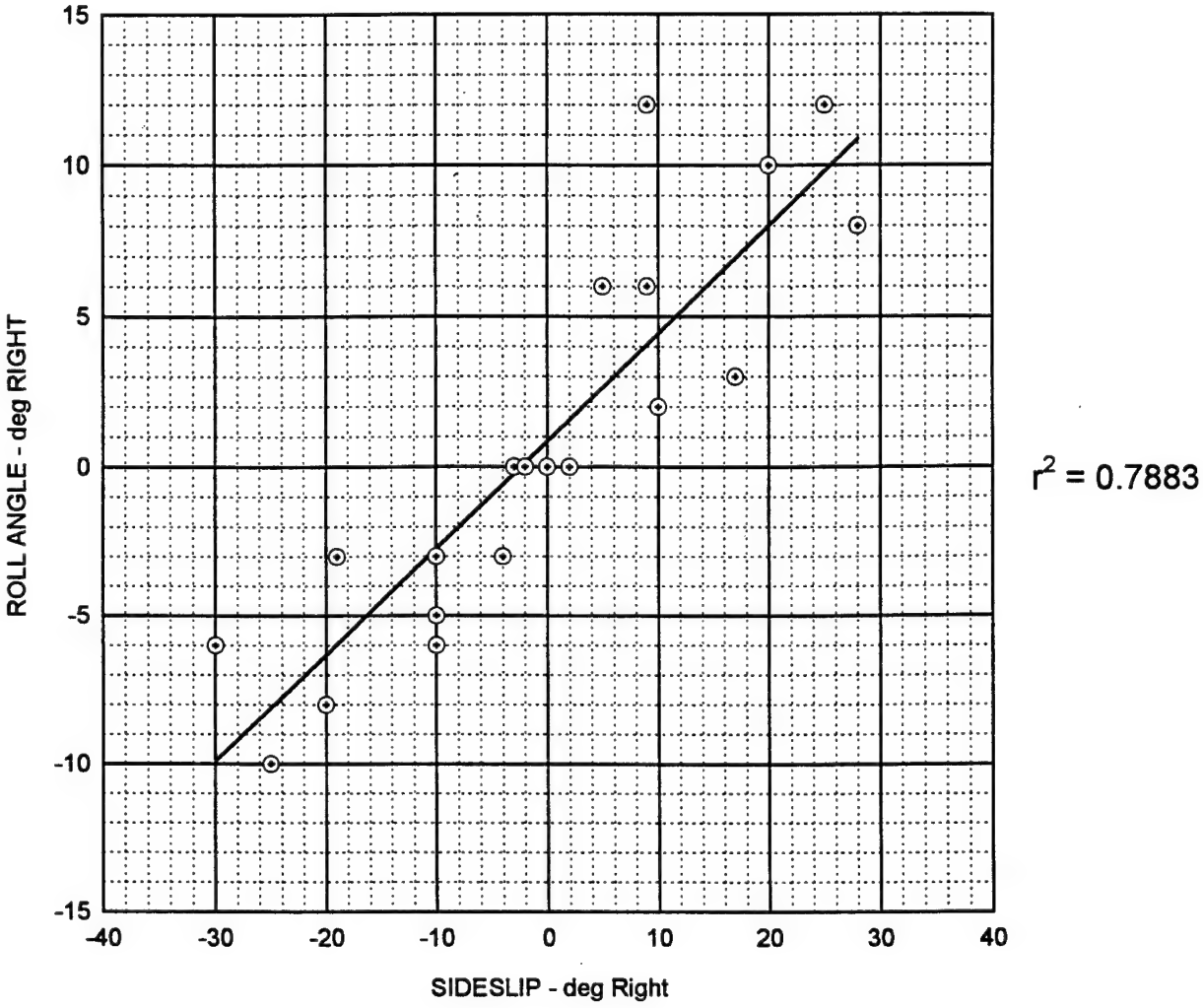

Figure A-7
MH-53E SIDESLIP VERSUS ROLL ANGLE

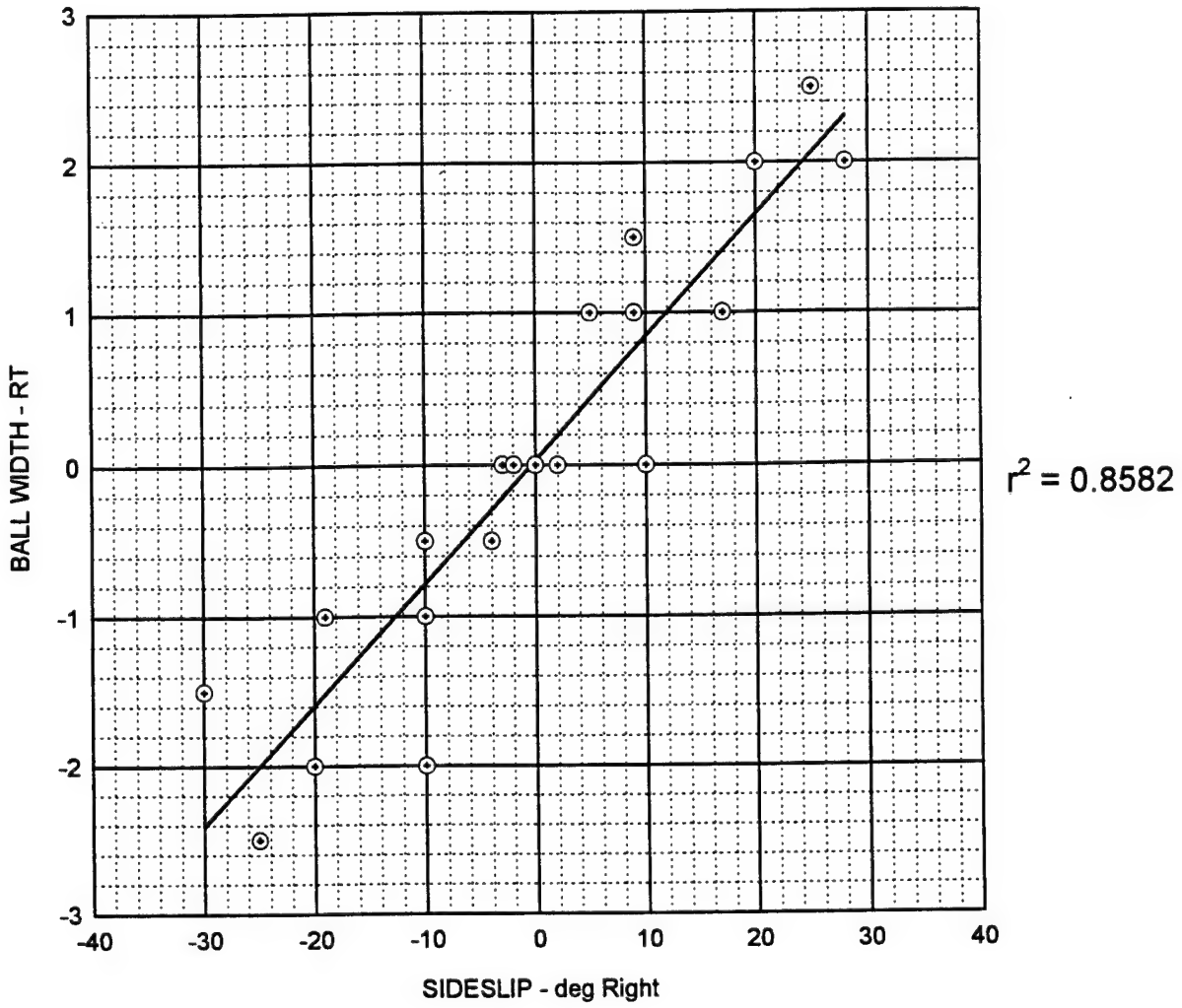

Figure A-8
MH-53E SIDESLIP VERSUS BALL WIDTH

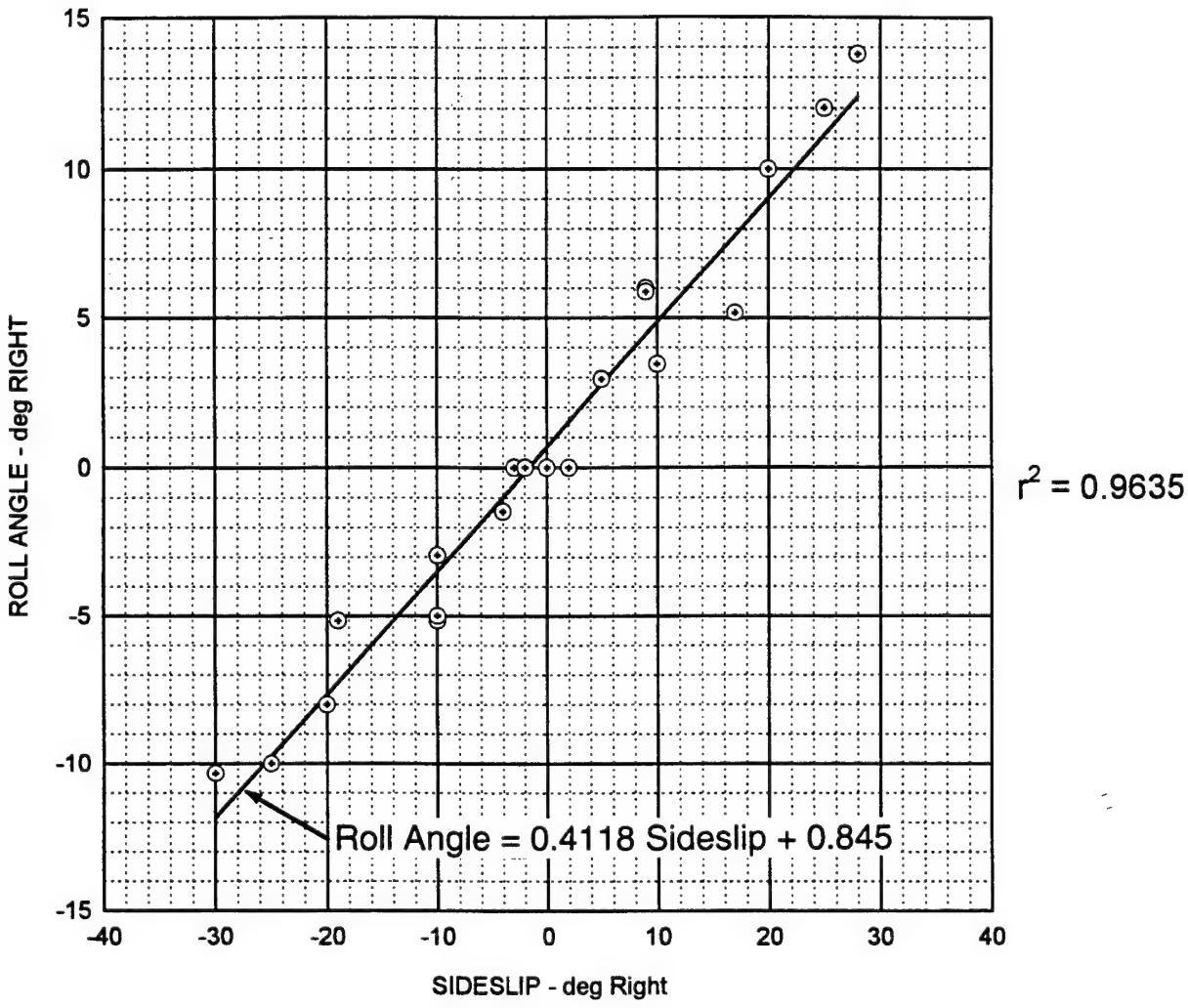

Figure A-9
MH-53E ROLL ANGLE VERSUS SIDESLIP
(CORRECTED FOR DYNAMIC PRESSURE (q) TO 105 KIAS)

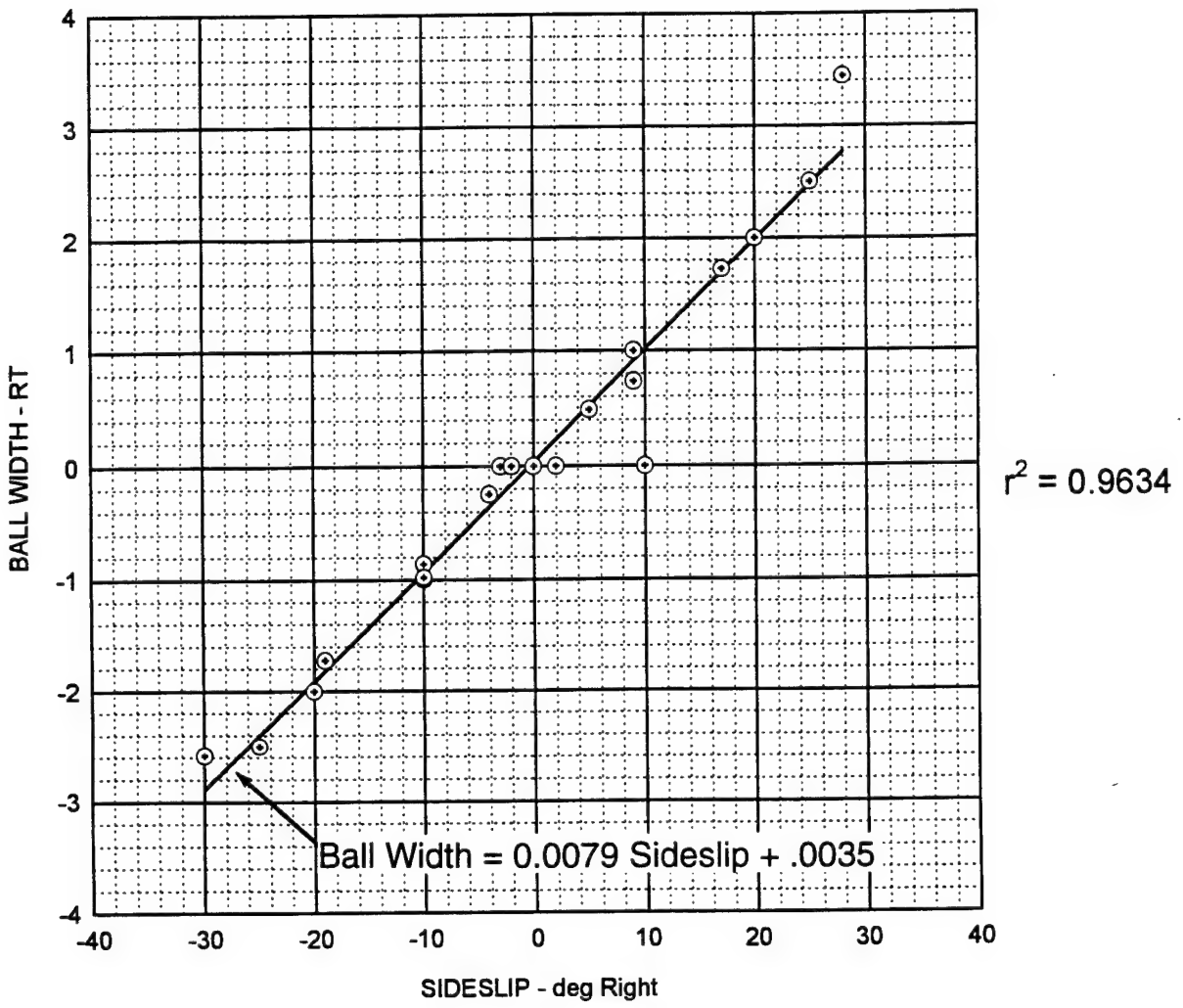

Figure A-10
MH-53E SIDESLIP VERSUS BALL WIDTH
(CORRECTED FOR DYNAMIC PRESSURE (q) TO 105 KIAS)

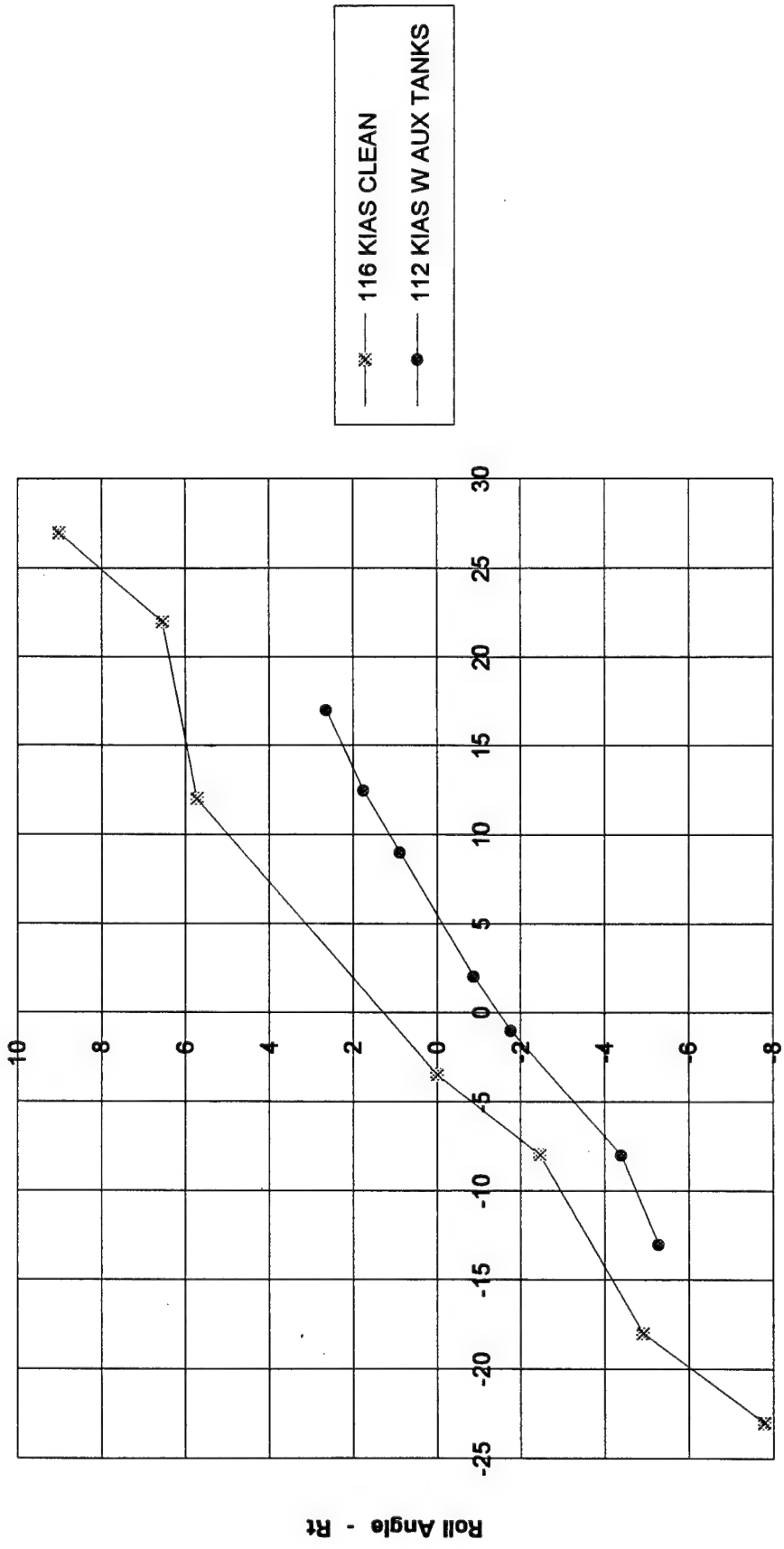

Figure A-11
CH-53E ROLL ANGLE VERSUS SIDESLIP

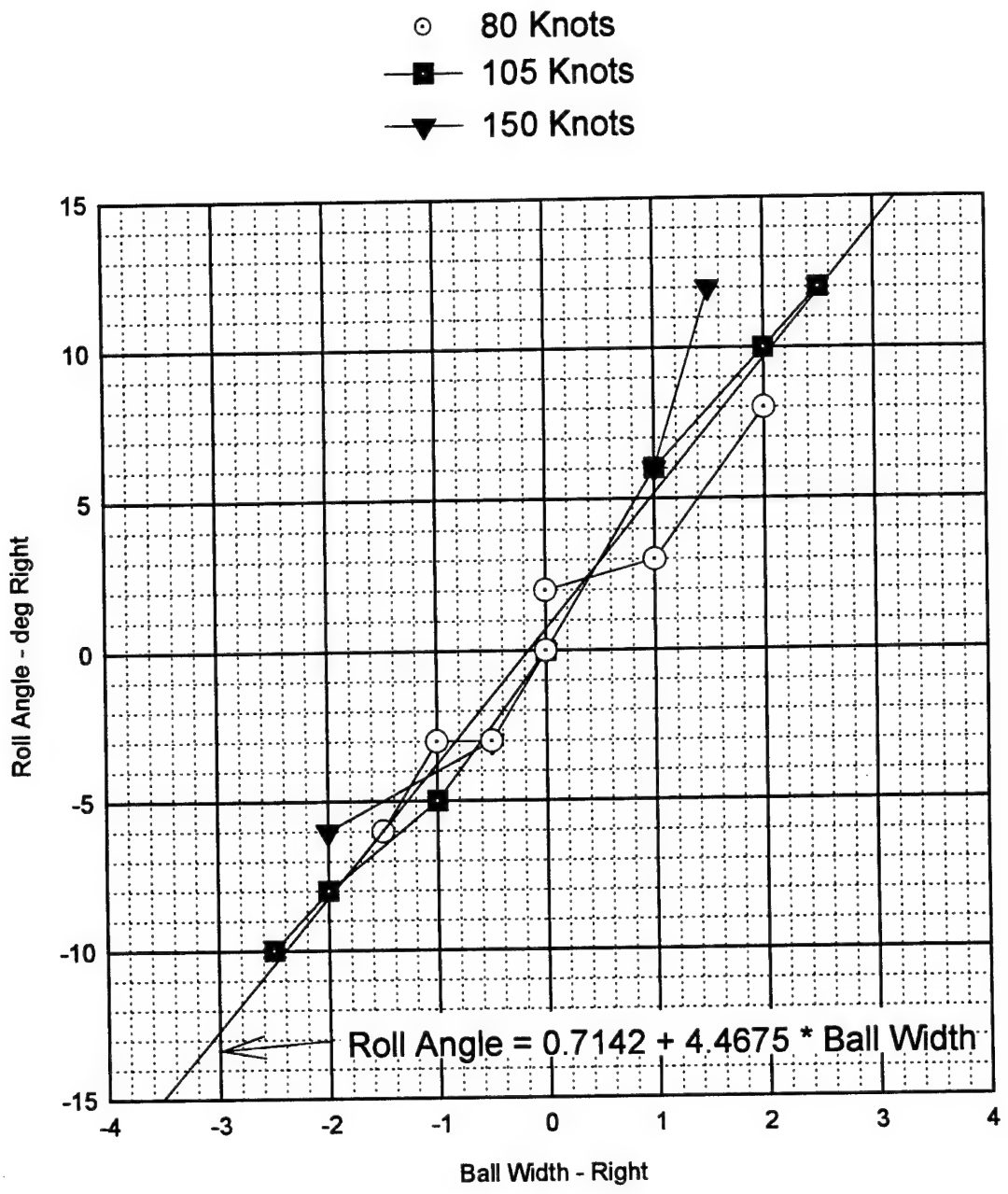

Figure A-12
MH-53E BALL WIDTH VERSUS ROLL ANGLE
(CALIBRATION PLOT)

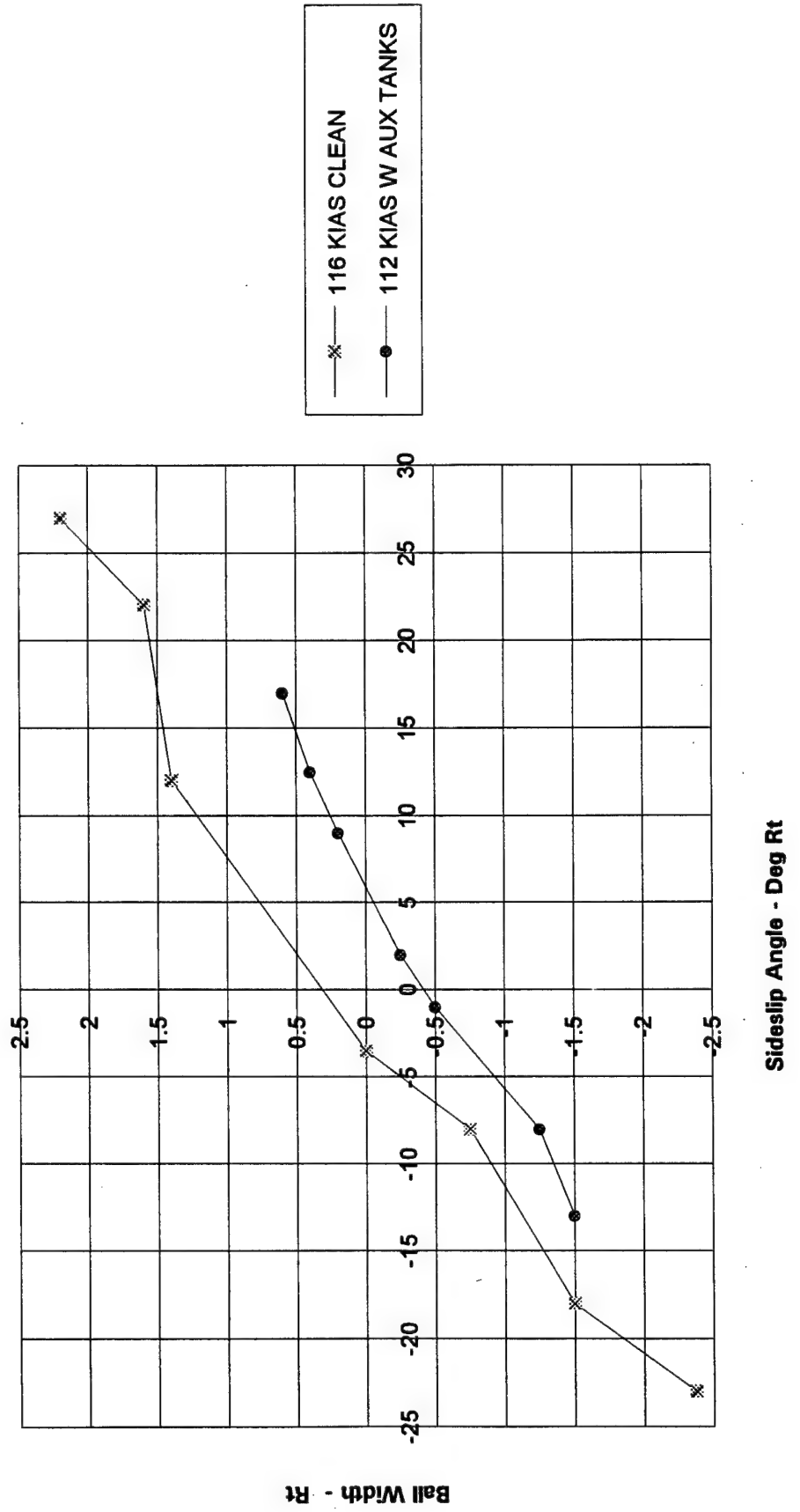

Figure A-13
CH-53E BALL WIDTH VERSUS SIDESLIP

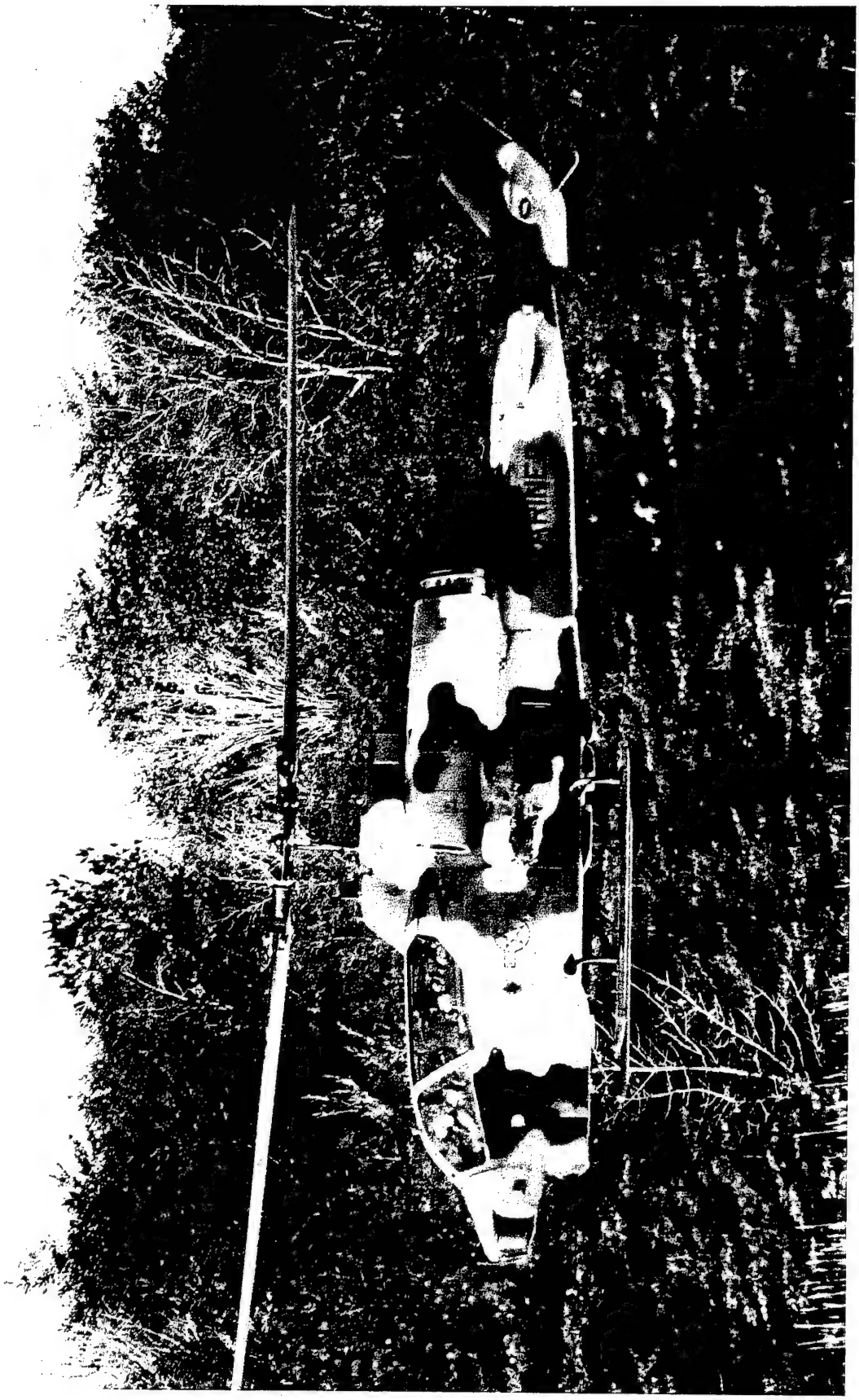

Figure A-14
AH-1W AIRCRAFT

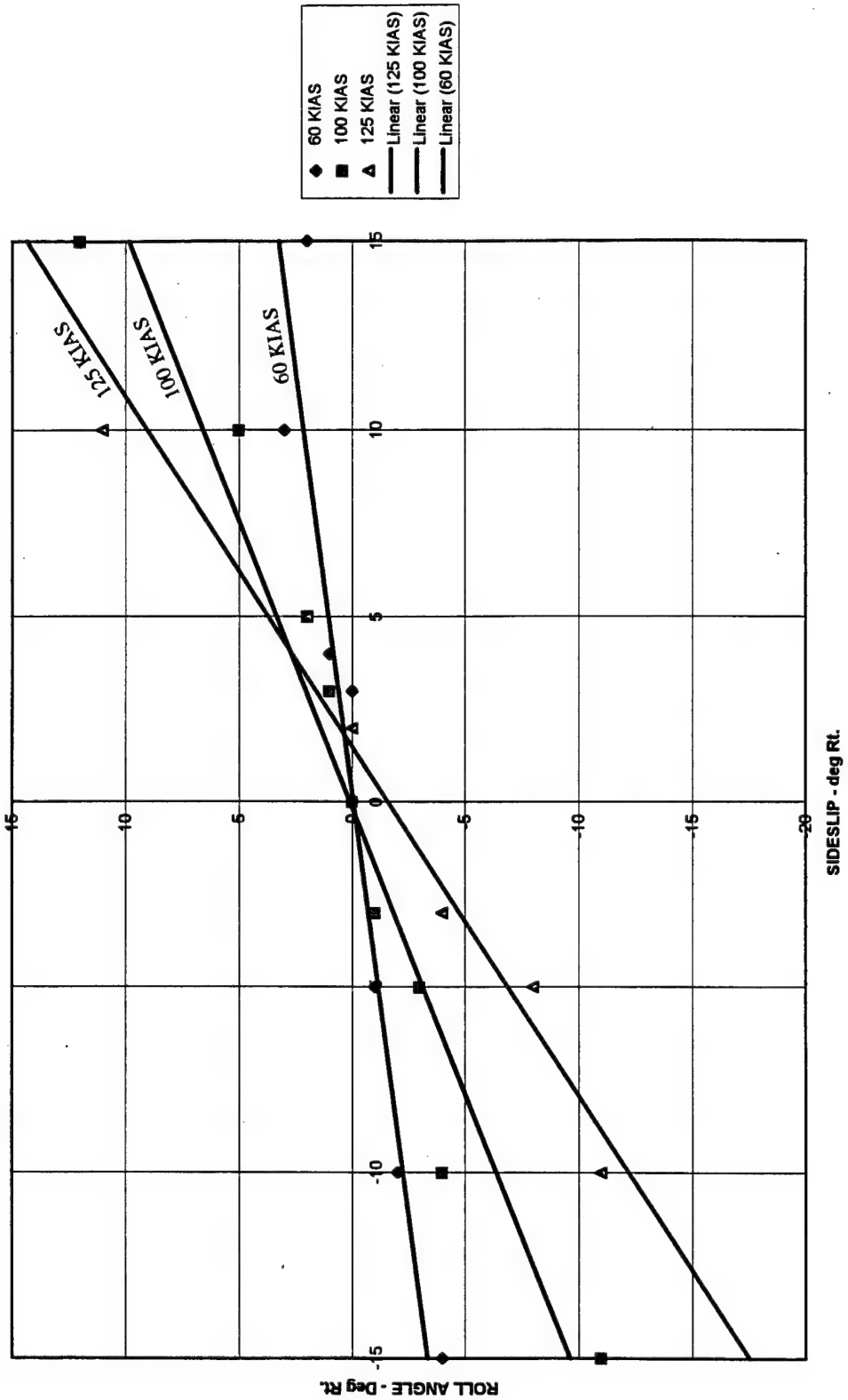

Figure A-15
AH-1W ROLL ANGLE VERSUS SIDESLIP - SCAS ON

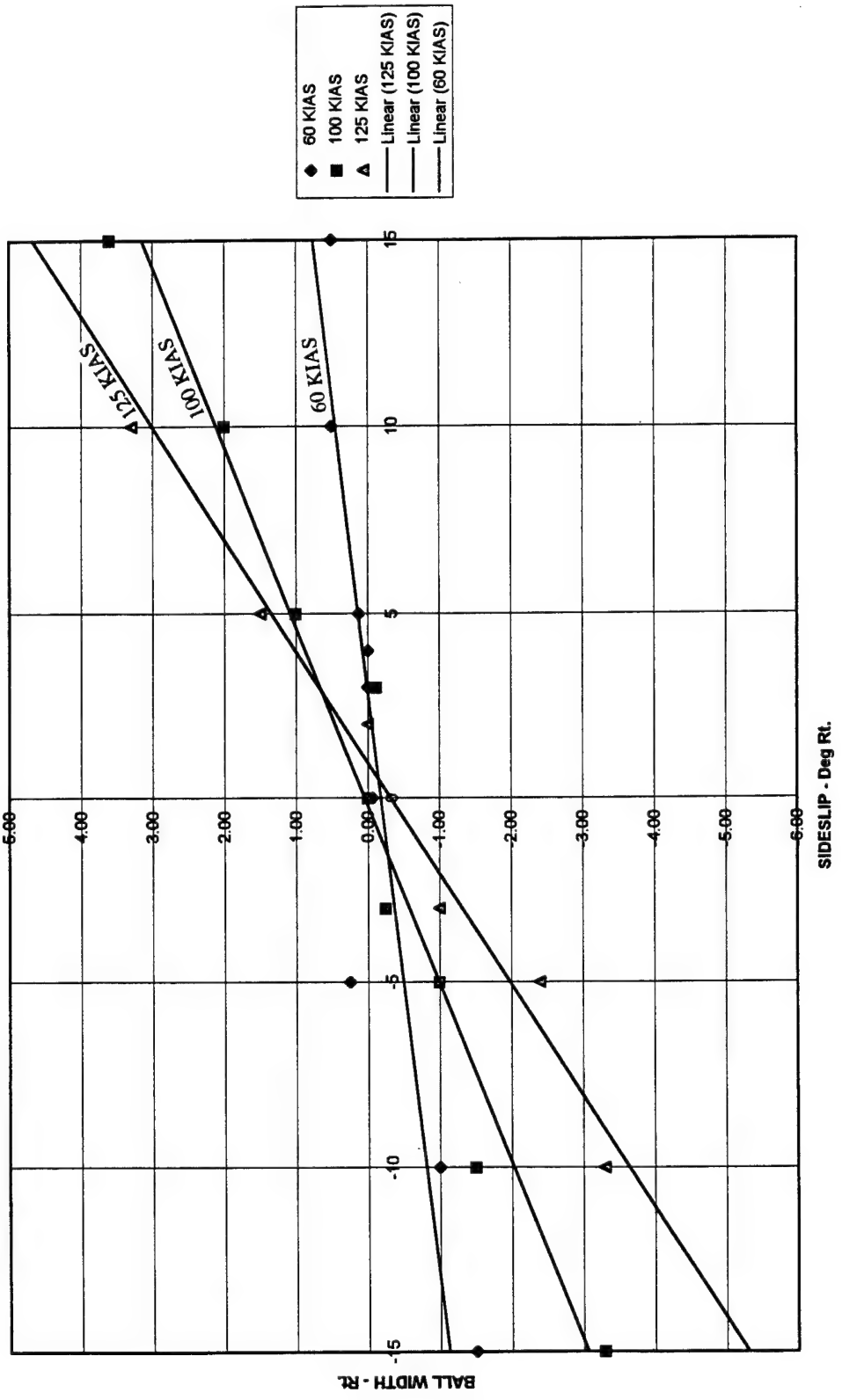

Figure A-16
AH-1W BALL WIDTH VERSUS SIDESLIP - SCAS ON

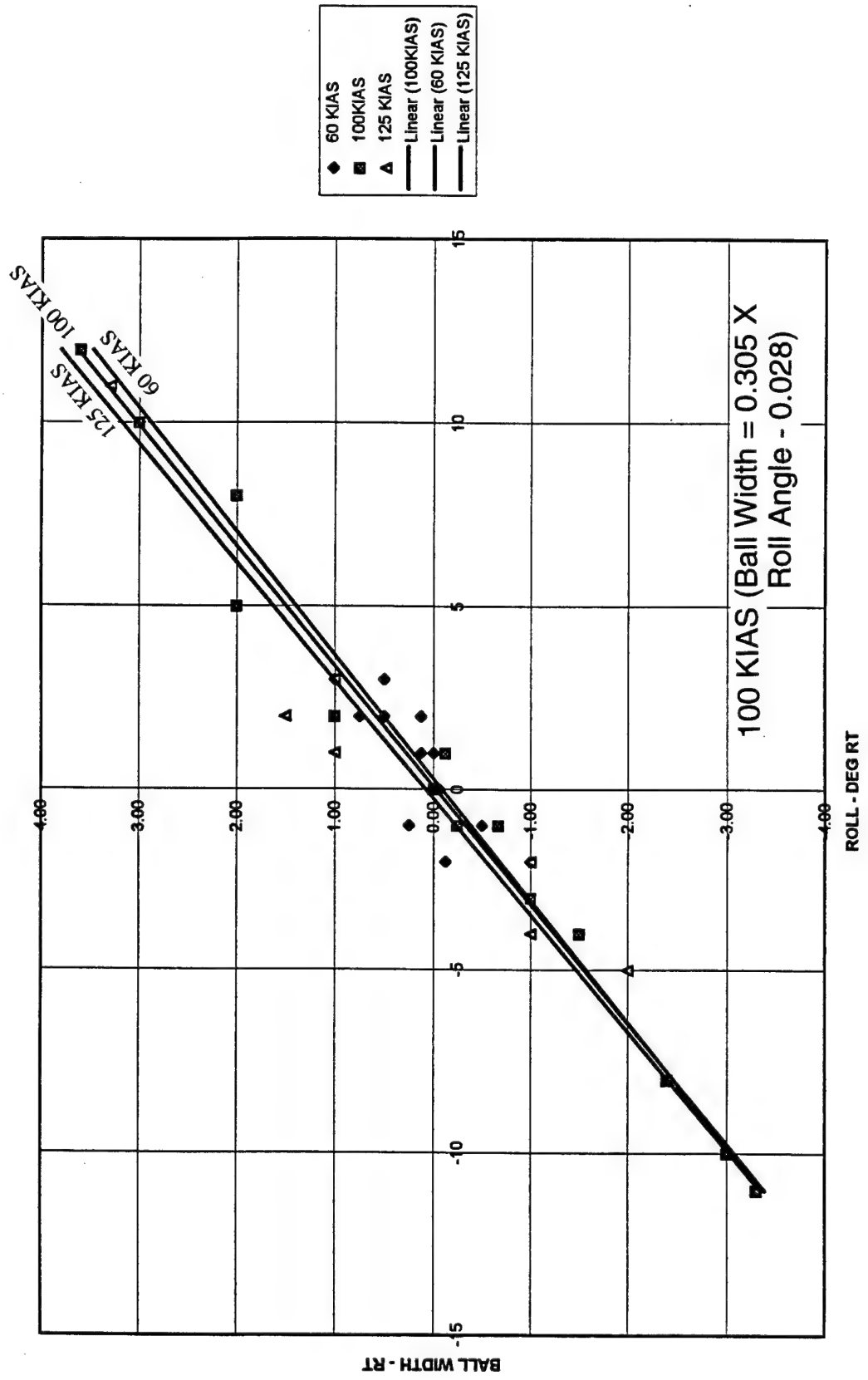

Figure A-17
AH-1W ROLL ANGLE VERSUS BALL WIDTH
(CALIBRATION PLOT)

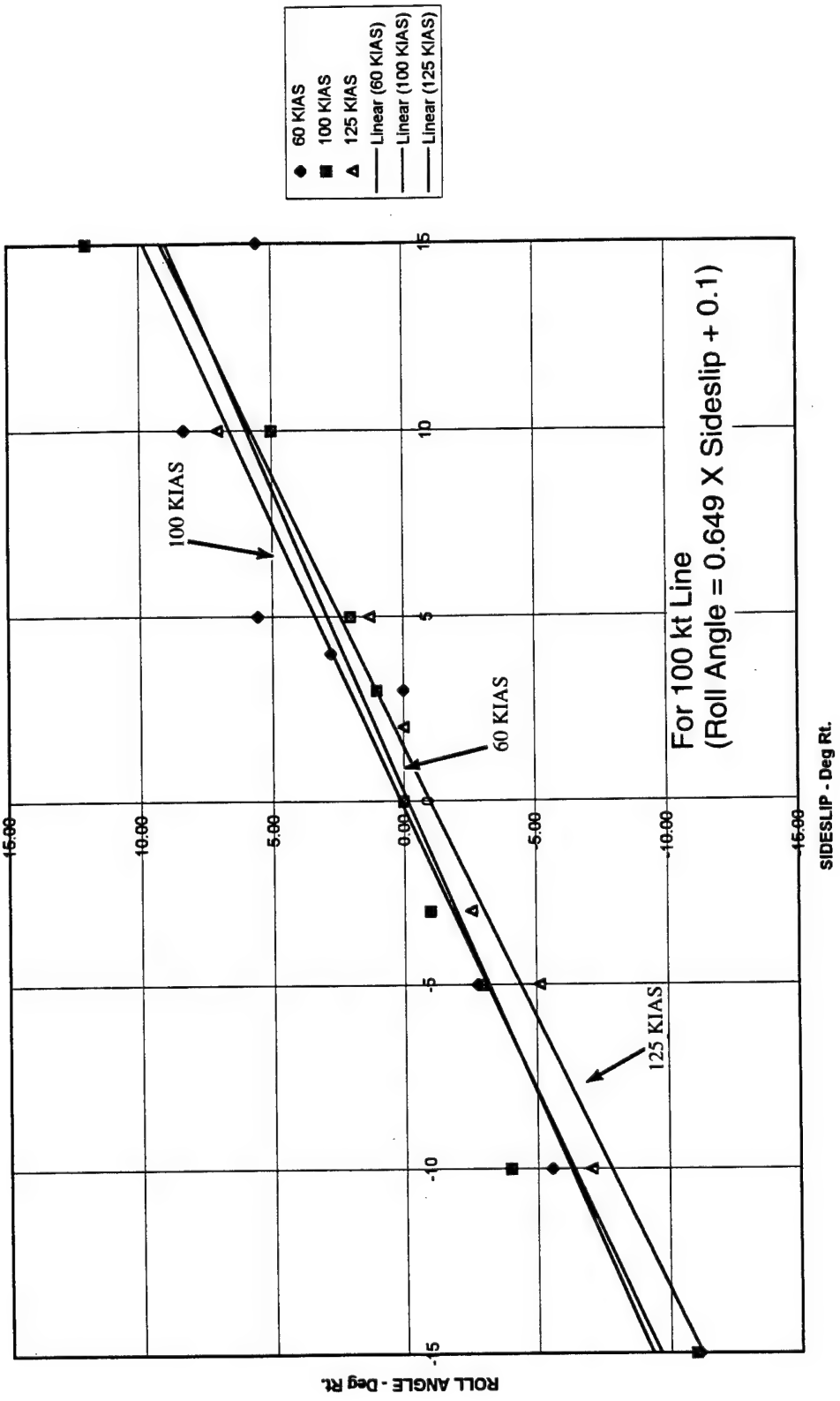

Figure A-18
AH-1W ROLL ANGLE VERSUS SIDESLIP - NORMALIZED TO 100 KIAS - SCAS ON

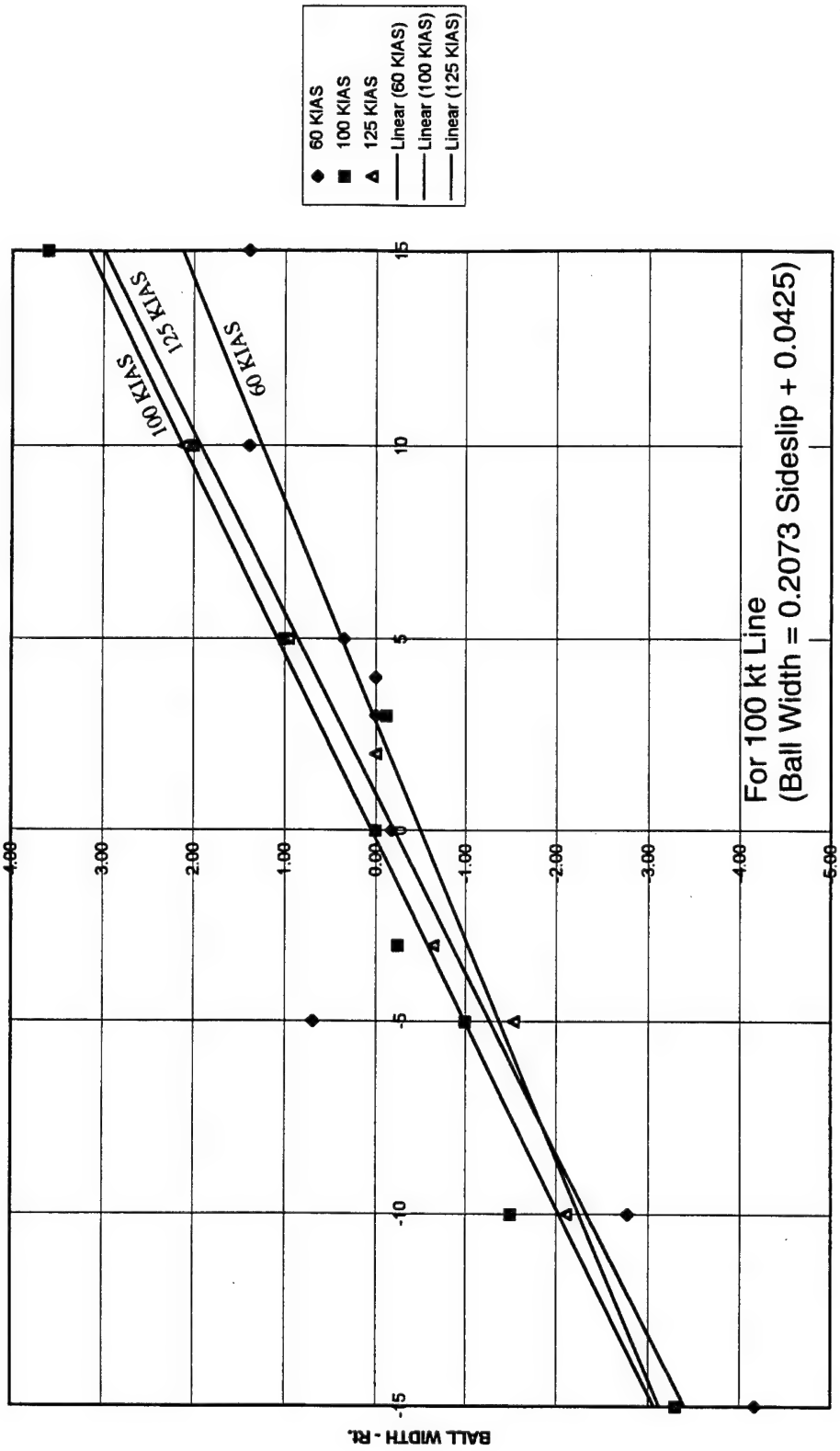

Figure A-19
AH-1W BALL WIDTH VERSUS SIDESLIP - NORMALIZED TO 100 KIAS - SCAS ON

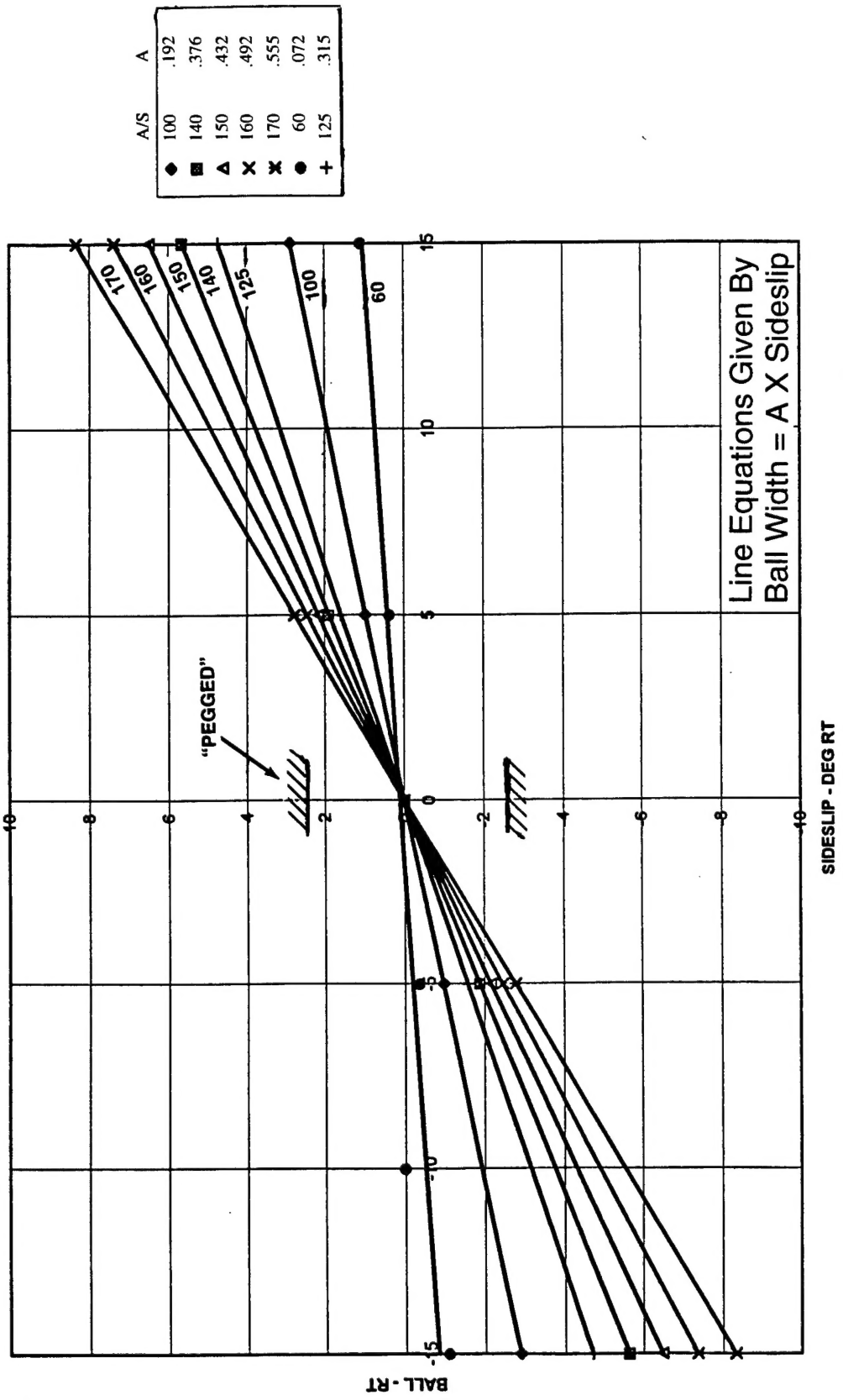

Figure A-20
COURSE BALL WIDTH WITH SIDESLIP

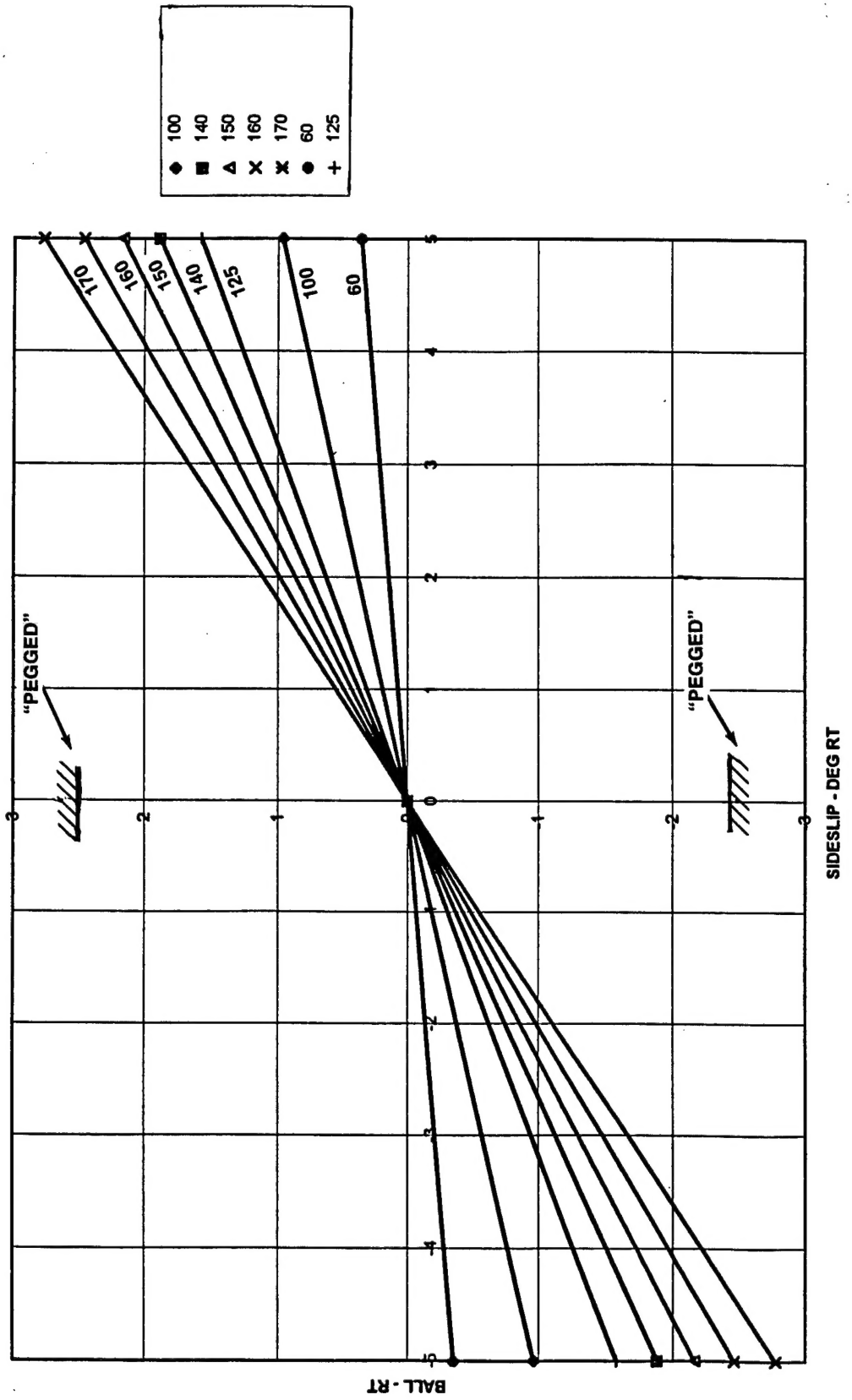

Figure A-21
FINE BALL WIDTH WITH SIDESLIP
(REFER TO FIGURE A-20 FOR LINE EQUATIONS)

THIS PAGE INTENTIONALLY LEFT BLANK

DISTRIBUTION:

INSURV AVIATION BOARD, Patuxent River, MD	(1)
NAVAIRSYSCOM (AIR-4.3)	(3)
NAVTESTWINGLANT Patuxent River, MD (55TW01A)	(1)
NAVRWAIRTESTRON Patuxent River, MD (55RW3SA)	(1)
NAVRWAIRTESTRON Patuxent River, MD (55RW10A-SOA)	(2)
NAVRWAIRTESTRON Patuxent River, MD (55RW10A-DI)	(2)
NAVRWAIRTESTRON Patuxent River, MD (55RW10A-H57)	(2)
NAVRWAIRTESTRON Patuxent River, MD (55RW10A-H60F)	(1)
NAVRWAIRTESTRON Patuxent River, MD (55RW10A-HH60H/J)	(1)
NAVRWAIRTESTRON Patuxent River, MD (55RW10A-H60B)	(1)
NAVRWAIRTESTRON Patuxent River, MD (55RW10A-VH)	(1)
NAVRWAIRTESTRON Patuxent River, MD (55RW10A-SP(H2/H3)	(1)
NAVRWAIRTESTRON Patuxent River, MD (55RW10A-UH1)	(1)
NAVRWAIRTESTRON Patuxent River, MD (55RW10A-AH1)	(1)
NAVRWAIRTESTRON Patuxent River, MD (55RW10A-H46)	(1)
NAVRWAIRTESTRON Patuxent River, MD (55RW10A-H53)	(3)
NAVRWAIRTESTRON Patuxent River, MD (55RW10A-V22)	(1)
NAVTESTPILOTSCH Patuxent River, MD	(2)
NAVAIRWARCENACDIV Patuxent River, MD (4.11)	(1)
NAVAIRWARCENACDIV Patuxent River, MD (4.11.1)	(2)
NAVAIRWARCENACDIV Patuxent River, MD (4.11.1.2)	(2)
NAVAIRWARCENACDIV Patuxent River, MD (4.11.1.3)	(2)
NAVAIRWARCENACDIV Patuxent River, MD (4.11.1.4)	(2)
NAVAIRWARCENACDIV Patuxent River, MD (4.11.1.5)	(2)
NAVAIRWARCENACDIV Patuxent River, MD (Technical Publishing Team)	(2)
NAVAIRWARCENACDIV Patuxent River, MD (RWV22.EB)	(3)
DTIC	(4)